Highlights

Unravelling the ultrafast dynamics of a N-BODIPY compound

Sandra Doria,Maria Taddei,Lorenzo Cupellini,Giacomo Biagiotti,Paolo Bartolini,Laura Bussotti,Stefano Cicchi,Paolo Foggi,Benedetta Mennucci,Mariangela Di Donato

- Ultrafast behavior of N-BODIPY highly dependent on solvent polarity
- Partial kasha rule violation and fluorescence emission from S2 electronic state
- Combined computational and spectroscopic methods to identify charge transfer and localized states involved in the excited state dynamics
- Fluorescence quenching in polar solvents due to photoinduced electorn transfer

Unravelling the ultrafast dynamics of a N-BODIPY compound

Sandra Doria[a,b], Maria Taddei[b], Lorenzo Cupellini[d,**], Giacomo Biagiotti[c], Paolo Bartolini[b], Laura Bussotti[b], Stefano Cicchi[c], Paolo Foggi[e,b,f], Benedetta Mennucci[d] and Mariangela Di Donato[a,b,*]

[a]*ICCOM-CNR, via Madonna del Piano 10, I-50019 Sesto Fiorentino (FI), Italy*
[b]*LENS (European Laboratory for Non-Linear Spectroscopy), Via N. Carrara 1, 50019 Sesto Fiorentino, FI, Italy.*
[c]*Dipartimento di Chimica "Ugo Schiff", Universitá degli Studi di Firenze, via della Lastruccia, 3-13, 50019 Sesto Fiorentino, Florence, Italy*
[d]*Dipartimento di Chimica e Chimica Industriale, Universitá di Pisa, via G. Moruzzi 13, 56124, Pisa, Italy*
[e]*Department of Chemistry, Biology and Biotechnology, Centro di Eccellenza sui Materiali Innovativi Nanostrutturati (CEMIN), University of Perugia, via Elce di Sotto 8, Perugia, 06123, Italy*
[f]*INO-CNR, Largo Fermi 6, Firenze, 50125, Italy*

ARTICLE INFO

Keywords:
N-BODIPY
Transient Absorption Spectroscopy
Charge transfer states
DFT computations

ABSTRACT

Although the photophysics of BODIPY compounds has been widely investigated in the last few years, their analogue N-BODIPY compounds, with nitrogen substitution at the Boron center, did not receive comparable attention. In this work we report about the systhesis and photochemical characterization of a substituted N-BODIPY compound, by means of a combined theoretical and spectroscopic approach. Compared to a standard BODIPY, the compound under investigation presents a lower fluorescence quantum yield (QY) in the visible region. The excited state relaxation dynamics of the dye was studied in different solvents, showing further fluorescence quenching in polar solvents, and a excited state decay rates strongly dependent on the environment polarity. The role of the pendant moieties and the involvement of charge transfer states in the excited state dynamics was experimentally addressed by transient absorption spectroscopy, and further analyzed with TD-DFT calculations, which allowed precise assignment of the transient signals to the correspondent electronic configuration. The complete picture of the N-BODIPY behavior shows the presence of both charge transfer and localized states, influencing the observed photophysics to different amounts, depending on the excitation conditions and the surrounding environment.

1. Introduction

Boron(III) dipyrromethene (BODIPY) compounds have been largely reported in literature and employed in a variety of applications thanks to their unique properties: chemical robustness, thermal resistance, low photodegradation, good solubility in organic solvents and penetration in cell membranes, intense molar extinction coefficients and good fluorescence quantum yields in the visible spectrum [1, 2, 3, 4]. In addition, a variety of BODIPY design and synthetic strategies can be adopted to achieve the photopysical properties required for a specific purpose [1, 2, 5, 6, 7].

Different pendant moieties can be linked to the BODIPY core to optimize their performances as laser media, application that requires a large Stokes shift to avoid self-quenching, while maintaining a high degree of rigidity in the molecular structure to prevent photo-damage [8, 9, 10, 11, 12, 13]. Donor-acceptor systems can be realized to enhance resonance energy transfer (RET) mechanisms for light-harvesting antennas [14, 15, 16, 17, 18, 19] and photovoltaic cells [20, 21, 22, 23, 24, 25] applications. "Ad hoc" functionalization of the BODIPY core can be applied to finely control absorption and emission bands, inducing shifts up to the near IR region, which opens up the possibility to use these dyes as fluorescent probes for imaging in living cell. Finally, several BODIPY compounds have been documented to show reversible "on-off" photoinduced electron transfer (PET) activity [26, 27, 28, 29] depending on the surrounding environment (pH and solvent polarity) [5, 30, 31, 32, 33, 34, 35, 36, 11, 37, 38] which makes these dyes suitable for detection of metal-ions [39, 3] [40]. In the medical field BODIPYs can be employed also as intracellular redox monitoring systems [2, 41, 42, 43, 44, 45] and activators for photodynamic therapy [46, 47], by the introduction of the right substituents during synthesis.

Most synthetic routes are focused on substitutions of the indacene core at the *meso* position [48, 49, 50, 51, 52, 53], while the functionalization of the boron atom is still limited to fluorine atoms (F-BODIPY [54]), alkoxy or aryloxy moieties (O-BODIPY [55]) and alkyls or aryl moieties (C-BODIPY [56]) [50, 51, 52, 53, 57, 58]. Only recently, C. Ray et al. [59, 60] synthesized and characterized, in terms of photochemical properties, a library of N-BODIPY chromophores, paving the way for testing new pendant moieties and extending the potential of this family of dyes. Depending on the chemical design, they observed different fluorescence properties, due to the predominance of either RET or PET.

In this work we synthesize and characterize, by means of stationary and ultrafast spectroscopic techniques, a N-BODIPY dye, containing a *para*-nitrophenyl group in the *meso* position and a diamino-boron substituent with two tosyl pendant

*Principal corresponding author
**Corresponding author
lorenzo.cupellini@unipi.it (L. Cupellini); didonato@lens.unifi.it (M.D. Donato)
ORCID(s): 0000-0002-9440-1643 (S. Doria)

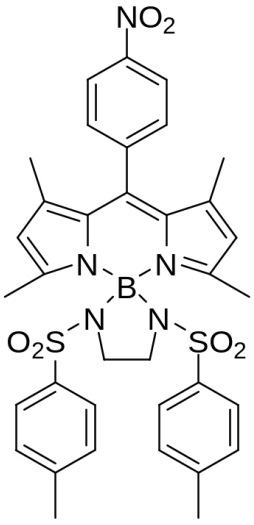

Figure 1: *Chemical structure of compound **1***

moieties on the opposite side of the BODIPY core ((compound **1**, chemical structure in FIg. 1). A similar structure, lacking however of the *meso* nitrophenyl substituent, has been already studied in reference[59]. Previous studies on the parent compound lacking of the *meso* group, demonstrated that the molecule is highly fluorescent in a variety of solvents, and at the solid sate. On the contrary, our molecule has a lower fluorescence quantum yield, that results almost completely quenched in polar solvents. Ray et al. [59] suggested that the presence of the diamono-boron appendant could induce the stabilization of a charge transfer state, responsible for the fluorescence quenching. However, in the particular case of the chromophore studied in this work, we propose the formation of a charge transfer state involving the nitrophenyl group, on the basis of a combination of experimental and theoretical analysis. Furthermore, we also find that the excited state lifetime and fluorescence yield of our chromophore depend on the excitation wavelengths, partially violating the Kasha rule.

We interpret the experimental observations in terms of a modulation of the energy of the frontier orbitals localized on the different molecular moieties by the polarity of the solvent, and rationalize the changes in the relaxation kinetics observed under different excitation conditions on the basis of the nature and energies of the higher excited states of the molecule, as retrieved from TD-DFT computations.

2. Experimental methods

2.1. Synthesis procedure

The synthesis procedure is schematized in Fig. 2. A 25 ml round bottomed flask under nitrogen atmosphere was charged with a solution of nitro-Bodipy (X) (52 mg, 0.141 mmol) in dichloromethane (DCM) (8 mL). a 1 M solution of BCl3 in DCM (0.26 mL) was added, dropwise and under stirring. A TLC control (1:1 DCM:Pet. Et.) showed a spot at $R_f = 0.37$. After 1 h, dry triethylamine (0.16 mL,

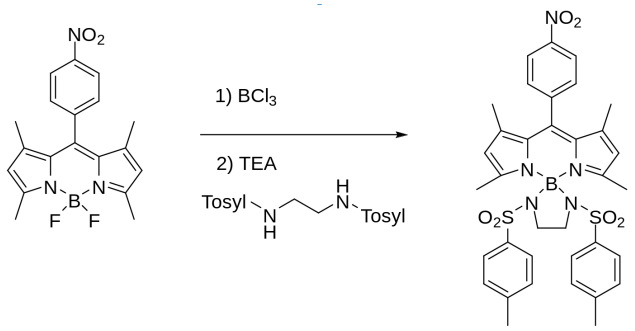

Figure 2: *Scheme of synthesis procedure of the N-BODIPY compound.*

1.1 mol) and N,N'-ditosyl-ethylendiamine (152.2 mg, 0.413 mmol) were added and the solution immediately turned into a deeper red color. The reaction mixture was left under stirring overnight and checked by TLC showing a spot at R_f = 0.10. The reaction mixture was filtered over a celite pad and concentrated under vacuum. The crude reaction mixture was purified by flash column chromatography (1:1 Pet. Et. : AcOEt, Rf = 0.29) to obtain 19 mg of the final product (yield 19 %). NMR results are described in SI.

2.2. Spectroscopic instrumentation

Linear spectroscopy. UV–Vis absorption and fluorescence spectra were recorded with a Perkin Elmer Lambda 950 UV–Vis spectrophotometer and a Perkin Elmer LS55 spectrofluorimeter, respectively. Fluorescence quantum yield (QY) has been measured with a Jasco FP-8300, instrument equipped with an integrating sphere ILF-835, which allows the determination of the absolute quantum yield without the need of an external standard. Measurements have been performed using a quartz cell with 1 mm optical path. All the analyzed solutions had an approximate absorption of 0.1 OD at the excitation wavelength.

Ultrafast spectroscopy. The ultrafast spectroscopy setup used in this work is based on a home-made Ti:sapphire laser oscillator. The short pulses produced by the oscillator (70 fs) are stretched and amplified at 1 kHz repetition rate by a regenerative amplifier (Amplitude Pulsar), pumped by a neodymium-doped YLF ($Nd^{3+} : YLF$) laser, frequency doubled intracavity to emit at 523.5 nm. After compression, pulses centered around 800 nm, with a total average power of 450-500 mW and duration of 100 fs are obtained.

Excitation pulses at 500 nm are obtained by non linear frequency mixing the signal output of a TOPAS apmplifier (Traveling wave Optical Parametric Amplifier of Superfluorescence, Light Conversion) with a portion of the 800 nm pump pulse in a BBO crystal. Pump pulses at 350 nm are instead obtained generating the fourth harmonic of the signal produced by the TOPAS. The probe beam, consisting in a white light continuum, is generated by focussing a portion of the fundamental radiation at 800 nm in a 3 mm thick Calcium Fluoride plate. Pump and probe beams are focussed and overlapped at the sample position. After passing through the

sample, the pump beam is blocked, while the probe is sent to the detector. Multichannel detection for transient spectroscopy is achieved by means of a flat field monochromator coupled with a home-made CCD detector. Pump-probe delays are introduced by sending the probe beam through a motorized stage. Measurements were carried out in a quartz cell (2 mm optical path length) mounted on a movable stage to avoid sample photo-degradation and photoaccumulation of long-lived species. The transient spectra were recorded in the spectral region between 350 and 750 nm. The recorded kinetic traces and transient spectra have been analysed by global-analysis [61]. The number of kinetic components has been estimated by performing a preliminary singular values decomposition (SVD) analysis [62]. Global analysis was performed using the GLOTARAN package (http://glotaran.org), [63] using a unidirectional a sequential kinetic scheme.

2.3. Computational methods

A (TD)DFT strategy was used to compute and characterize the excited states of the N-BODIPY in n-hexane and acetonitrile solvents. The N-BODIPY structure was optimized at the B3LYP/6-31G(d) level of theory. Excited states were computed with the long-range corrected ωB97X-D functional [64, 65] and the 6-31+G(d) basis set. The chosen functional reproduces the correct asymptotic $1/R$ behaviour of long-range charge-transfer excitations [66, 67, 68, 64], and gives similar results to B3LYP for the first bright excitation of N-BODIPY. Excited states were characterized by analyzing the natural transition orbitals (NTO), which provide a compact representation of the electronic transition [69, 70]. The excitations with CT character were identified with a NTO-based metric [71].

The solvent effects were introduced at all stages with the polarizable continuum model in its integral equation formalism (IEFPCM), which treats the solvent as a homogeneous medium characterized by its static and optical dielectic constants. State-specific solvent corrections were computed in the so-called corrected linear response (cLR) method [72] for the CT states, which possess significant density reorganization.

The solvent (i.e. outer-shell) contribution to the reorganization energy was computed for CT states as the difference between excitation energies computed with equilibrium and nonequilibrium solvation. In the nonequilibrium model, only the "fast" solvation, governed by the optical dielectric constant, is allowed to relax in response to the excitation, whereas the rest of the solvent polarization remains frozen to its ground-state configuration. In the equilibrium model, all solvation is relaxed to the excited state.

In order to compute the electronic couplings between excited states, we used a diabatization scheme [73] which is able to separate the excited-state manifold into locally excited and CT subspaces. The electronic Hamiltonian is then transformed in the diabatic basis to extract the off-diagonal electronic couplings.

3. Results and discussion

3.1. Linear spectroscopy

The absorption and emission spectra (excitation at 480 nm) of the N-BODIPY compound **1** dissolved in n-hexane, toluene, dichloromethane (DCM) and acetonitrile (ACN) are shown in Fig. 3a and 3b, respectively. In toluene the absorption spectrum is characterized by an intense band centered at 508 nm with a shoulder assigned as a vibronic band on its blue side (around 480 nm). A blueshift of about 5 nm is observed in dichloro-methane and hexane, that increases up to 10 nm in acetonitrile. An additional high-frequency absorption component is present below 400 nm.

The emission spectra, normalized respect to the optical density of the samples at the excitation wavelength (480 nm), are characterized by a broad band centered around 540 nm in toluene, which shifts at lower wavelengths in n-hexane (532 nm). In dichloromethane and acetonitrile, the fluorescence of the compound is strongly quenched. Furthermore, compared to a standard BODIPY, the fluorescence band of this molecule is broader, presents a higher Stokes shift and lacks the usually observed vibrational structure.[4, 74]. The fluorescence quantum yield of the compound is significantly lower if compared to a standard Bodipy: indeed a QY of only 11.5% is measured in toluene, which decreases to 6.8% in hexane and is almost totally quenched in more polar solvents (measured Qy are below unity in both solvents).

To further investigate emission properties of the sample, the fluorescence of compound **1** was quantitatively compared to that of a 1 to 1 mixture of a parent N-BODIPY lacking of diamino-tosyl substituent (but with *meso* nitrophenyl appendant) and the free di-tosyl amine, in different solvents. The results, reported in Fig. S1 of SI, show that the fluorescence of the *meso* nitrophenyl N-BODIPY without the diamino-tosyl substituents is still strongly quenched respect to that of a standard BODIPY, suggesting that the nitrophenyl group and not the nitrogen substituents determines the emission quenching. The emission of compound **1** is comparatively higher respect to the that of the 1 to 1 mixture, possibly because of an extended conjugation caused by nitrogen substituents.

Interestingly, if fluorescence is recorded by exciting the sample at 350 nm, a second blue shifted emission band of low intensity is observed, as shown in Fig. 4. In non polar solvents, two distinct fluorescence components are present: the already observed intense band at about 540 nm and a lower intensity component peaked at about 400 nm. In polar solvents the main fluorescence band is almost completely quenched, while the low intensity band is still observed. This behavior is unusual, since for the majority of organic molecules it is expected that fluorescence would occur always from the low laying excited state, in agreement with the Kasha rule. Furthermore, upon UV excitation the fluorescence QY decreases in polar solvents and increases in non-polar solvents, due to the slight rise of the high frequency fluorescence band in the latter media (a QY increase from 0.09% to 0.19% is measured in dichloromethane moving the excitation wave-

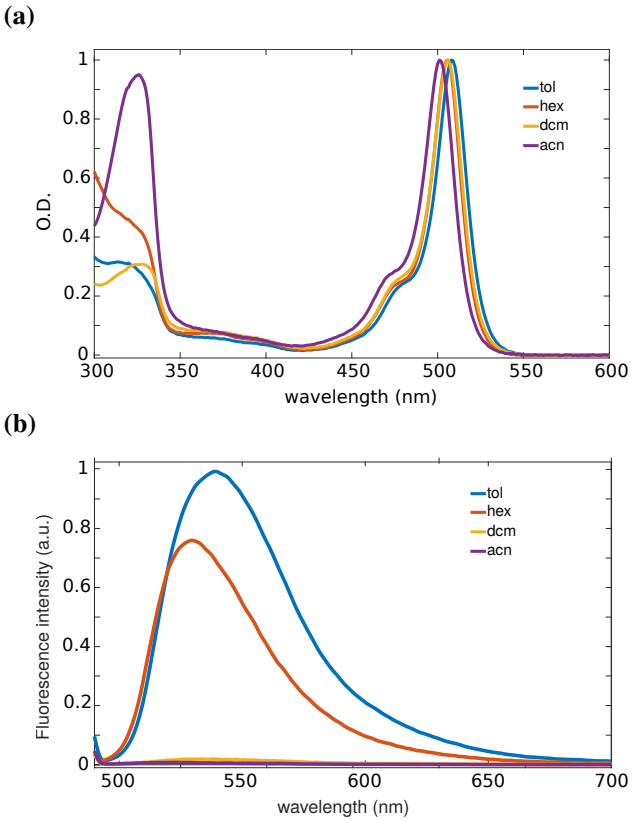

Figure 3: *a) Absorption spectra of the N-BODIPY compound in different solvents: toluene, n-hexane, dichloromethane and acetonitrile. b) Emission spectra of the compound in different solvents (excitation at 480 nm). The spectra are normalized respect to the optical density at the excitation wavelength.*

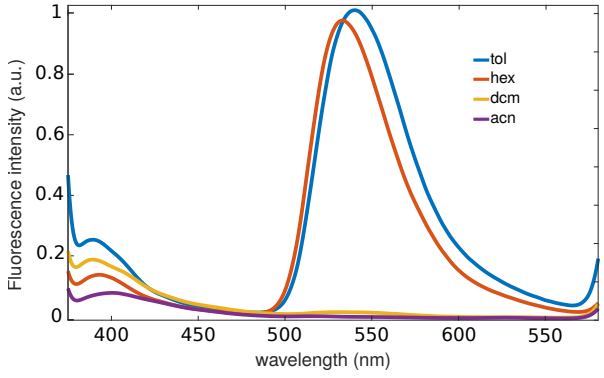

Figure 4: *Emission spectra of the compound recorded in different solvents, with excitation at 350 nm; the spectra are normalized respect to the optical density at the excitation wavelength.*

length from 480 to 350 nm).

3.2. Transient Absorption spectroscopy

Transient absorption spectroscopy (TAS) experiments have been carried out on the N-BODIPY compound dissolved in the four solvents considered in the previous section (n-hexane, toluene, dichloromethane and acetonitrile).

Fig. 5 shows the evolution associated difference spectra (EADS) extracted from a Global analysis performed on the kinetic traces (the experimental transient spectra are reported in Fig. S2a of SI) acquired for the compound in n-hexane, upon excitation at 500 nm. The linear absorption and emission spectra of the sample are shown on top of the EADS in Fig 5. The global analysis allows estimating three lifetimes of 356 fs, 13.1 ps and 383 ps, corresponding to the evolution of three spectral components which describe the excited state decay pathway of the sample, until the full recovery of the ground state population. The transient spectra are characterized by the appearance of a negative signal centered around 505 nm, with a broad tail extending up to 650 nm, which can be assigned as the convolution of ground state bleaching and stimulated emission. The stimulated emission rises on the red edge of the overall negative band in about 300 fs, as noticed by observing the spectral difference between the first two EADs, as the results of a rapid stabilization of the excited state reached upon vertical excitation. A small positive excited state absorption band is observed around 400 nm, which shows no remarkable spectral changes over time. The excited state evolution in toluene, shown in Fig. S4 of SI section is comparatively similar. When repeating the measurement in a more polar solvent, such as acetonitrile, notable differences are found, as shown in Fig.6

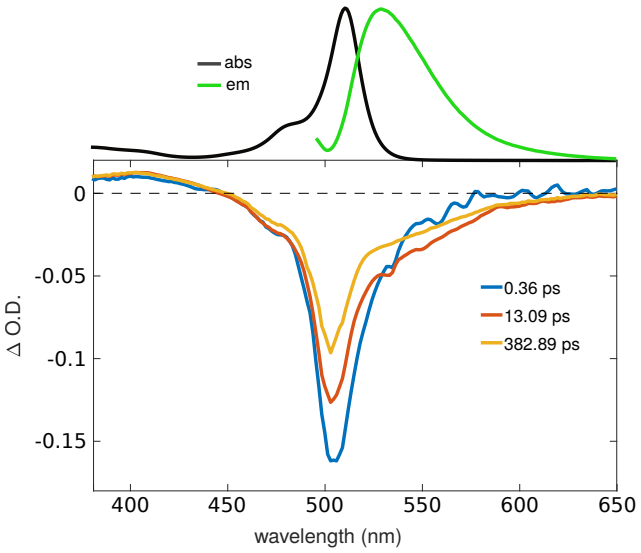

Figure 5: *EADS obtained by Global analysis performed on the kinetic traces collected in n-hexane upon excitation at 500 nm. The absorption and emission spectra are shown in the top panel.*

The EADS plotted in Figure 6 highlight a four-exponential decay described by lifetimes of 1.7 ps, 2.6 ps, 14.8 ps and 1 ns. The forth component has been added to increase the accuracy of the fit, but as noticed from Figure 6 it only accounts for a small background signal caused by the pump scattering. The overall excited state recovery is much faster than the one observed for non polar-solvents and the transient signal decays almost completely in about 15 ps. Besides time constants, also the evolution of the transient signal appears different from that previously described for non polar solvents.

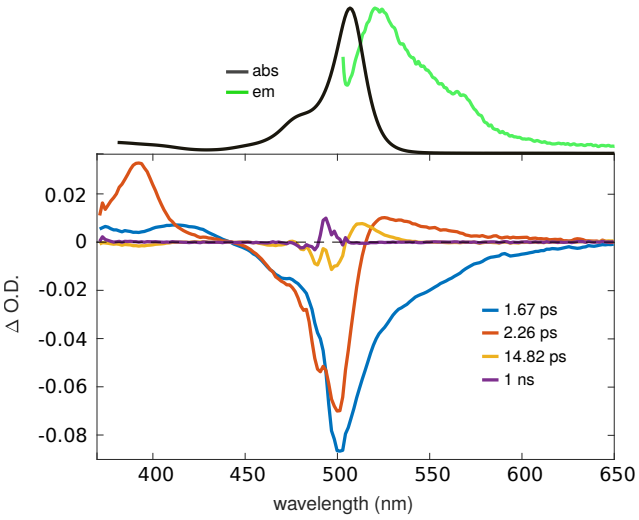

Figure 6: *EADS obtained by Global analysis performed on experimental transient spectra collected on the dyad in acetonitrile by excitation at 500 nm. Absorption and emission spectra are reported in the top panel*

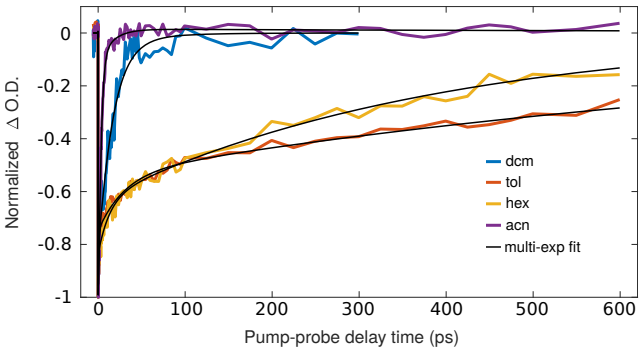

Figure 7: *Kinetics traces registered at the maximum of the bleaching signal (504 nm) in different solvents for excitation at 500 nm, superimposed to multi-exponential fit performed by global analysis*

Solvent	Polarity Index	τ_1	τ_2	τ_3	τ_4
n-Hex	0.1	0.36	13.1	383	–
Tol	2.4	0.74	30.0	938	–
Dcm	3.1	3.2	16.4	56	–
Acn	5.8	1.7	2.3	14.8	1000

Table 1
Time constants obtained by global fit of the transient data (500 nm pump).

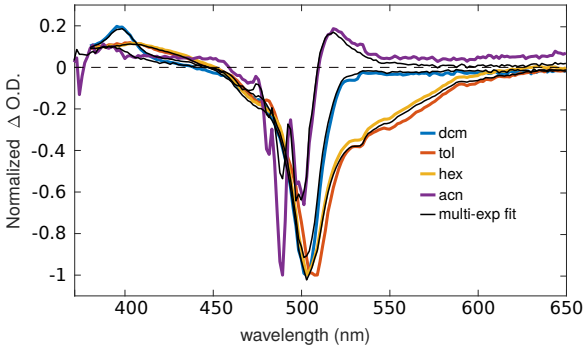

Figure 8: *Transient spectra recorded at a pump-probe delay time of 7.5 ps in different solvents and corresponding fit performed with Glotaran software, in case of 500 nm excitation wavelength.*

The initial EADS, with a lifetime of about 1.7 ps, is quite similar to that observed in hexane, but the evolution towards the second spectral component shows a noticeable decrease in intensity on the red side of the band, and the appearance of a small positive signal peaked at about 530 nm and of another positive peak at about 380 nm. Comparison with previous literature [75] allows to assign this component as due to the localization of a positive charge on the bodipy core. The formation of a charge separated state is supported by the computational studies described in the following section, which revealed the establishment of a charge transfer state between the *meso* nitrophenyl group and the bodipy core following the excitation.

In order to better understand the ultrafast behavior of the N-BODIPY compound **1** as a function of the solvent polarity, we plot in Fig. 7 the kinetic traces recorded at the wavelength corresponding to the maximum of the bleaching signal for all the four solvents tested, superimposed to the multi-exponential fit obtained with global analysis. It is possible to observe that the more polar is the solvent, the faster is the excited state decay, suggesting that a fast decay channel, which we assign to the population of a charge transfer state, is favoured by the increased polarity. A summary of the time constants describing the excited state evolution in the different solvents is reported in (Tab. 1) for the 500 nm excitation wavelength.

To further compare the influence of the solvent on transient spectral shapes and excited state evolution, we show in Fig 8 the transient spectra recorded at the fixed pump-probe time-delay of 7.5 ps, recorded in the four solvents tested. As it can be noticed, the transient spectra collected in the two non polar solvents n-hexane and toluene are very similar and, as previously mentioned, can be interpreted as the convolution of ground state bleaching (peak center around 500 nm) and stimulated emission (around 550 nm) signals. In the most polar solvent considered, acetonitrile, a positive band is clearly visible, peaked at about 530 nm, signaling the formation of a BODIPY cation. The spectral shape observed in dichlorometane, whose relative polarity is between that of toluene and acetonitrile (see also Tab 1), has an intermediate appearance: the red-shifted positive signal is barely visible, being almost totally compensated by the stimulated emission band. This could indicate that the CT yield is lower compared to more polare media.

In order to further investigate the observed excitation wavelength dependence of the sample fluorescence, we also

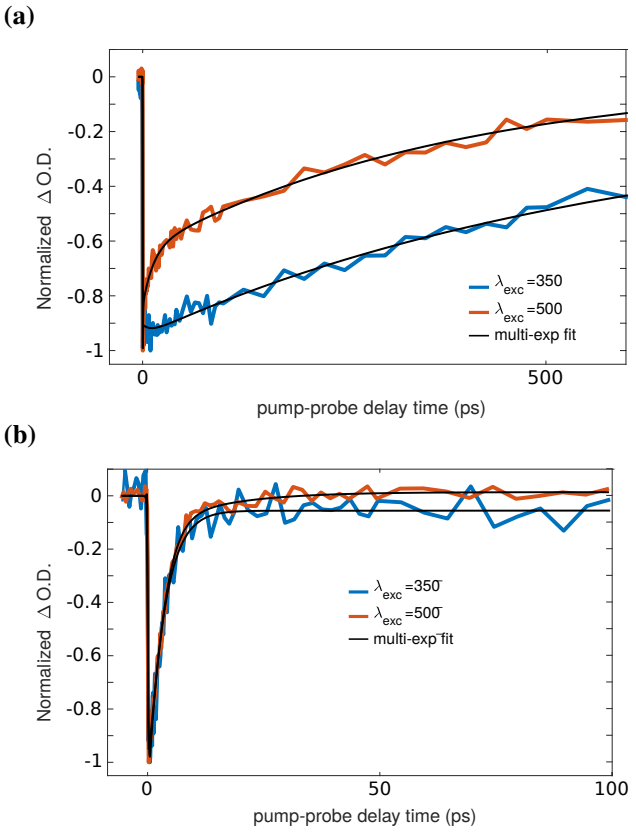

Figure 9: *Comparison between single wavelength kinetics (504 nm) of the dyad in hexane (a) and acetonitrile (b) by exciting at 350 and 500 nm, superimposed on corresponding multi-exponential fits obtained by global analysis.*

measured transient absorption spectra of the sample upon excitation at 350 nm. The transient data and their respective analysis are reported in SI.

The kinetic traces taken at the maximum of the bleaching signal in n-hexane and acetonitrile upon excitation at both 350 and 500 nm are compared in Figure 9.

The comparison of kinetic traces reported in Figure 9 clearly shows that the ground state recovery is faster upon excitation at 500 nm with respect to 350 nm excitation, especially in non-polar solvents. This observation suggests that different decay channels are activated upon UV excitation, possibly involving the decay towards an intermediate excited state characterized by a slower relaxation. Further evidence for the dependence of the excited state decay upon the excitation conditions can be inferred looking at the EADS reported in SI section.

The experimental observations of kinetic and spectral changes depending on the excitation wavelength could be explained by considering that different decay channels are involved in the dynamics at the two excitation wavelength. The observed behavior is not common for organic molecules, where usually the internal conversion between high energy excited state and the low lying S1 state is ultrafast. A possible explanation for the observed evolution is that upon excitation at 350 nm the system would decay towards an intermediate excited state highly localized on a peripheral substituent, thus weakly coupled with the S1 state localized on the N-BODIPY core. As shown in the following section, DFT computations support this explanation, since excited states completely localized on the nitro-phenyl substituent are located at intermediate energy between the S1 state and higher excited states localized on the N-BODIPY core.

	Acetonitrile		n-hexane		
State	ΔE (eV)	f	ΔE (eV)	f	Assignment
1	2.82	0.49	2.80	0.50	LE1
2	3.69	0.04	3.68	0.04	LE2
3	3.32[a]	0.0004	3.41[a]	0.0007	CT1
4	3.91	0	3.89	0	LE3[b]
5	4.05	0.10	4.04	0.09	LE4
6	4.52	0.02	4.66	0.02	LE5[c]
7	4.53[a]	0.0048	4.51[a]	0.0052	CT2
8	4.69	0.65	4.81	0.68	LE6[c]

[a] Energy corrected with the first-order cLR method (see Computational Methods)
[b] nitrophenyl $n \rightarrow \pi^*$ [c] nitrophenyl $\pi \rightarrow \pi^*$

Table 2
TD-DFT calculated excited states of N-BODIPY in acetonitrile and n-hexane solvents. Excitation enerrgy (ΔE) and oscillator strength are reported. The states are ordered by uncorrected energy in acetonitrile.

3.3. Computational results

In order to rationalize the spectra and dynamics of the N-BODIPY, we performed TD-DFT calculations in two solvents, the nonpolar n-hexane and the polar acetonitrile. The results (Table 2) support the assignment of the intense absorption band measured in the UV-Vis spectra to the BODIPY core. The natural transition orbitals (NTOs) indeed confirm that the excitation is well localized on the BODIPY moiety (Figure 10a). The discrepancy (~0.34 eV) between the calculated and experimental excitation energy is due to the well-known intrinsic difficulty of TD-DFT in describing the excited states of cyanine-like molecules.[76] The second BODIPY excited state is almost 1 eV higher in energy, and its intensity is an order of magnitude lower.

The calculations also predict a low-lying charge-transfer state, which is ~0.6 eV above the bright BODIPY state in n-hexane, and slightly lower in energy in acetonitrile. The dominant NTO pair involved in this state is reported in Figure 10b. Contrary to previous literature findings [59], this state does not involve the diamino-boron moiety, but it can be seen as an electron transfer from the BODIPY core to the nitrophenyl *meso* group.

A charge-transfer state involving the diamino-boron substituent can be found at ~4.5 eV, which is well above the low-lying states of the BODIPY. Figure 10c shows the dominant NTO pair for this state. Contrary to CT1, this transition is not a full electron transfer, as the hole and electron densities partially overlap. Due to its high energy, this state cannot be

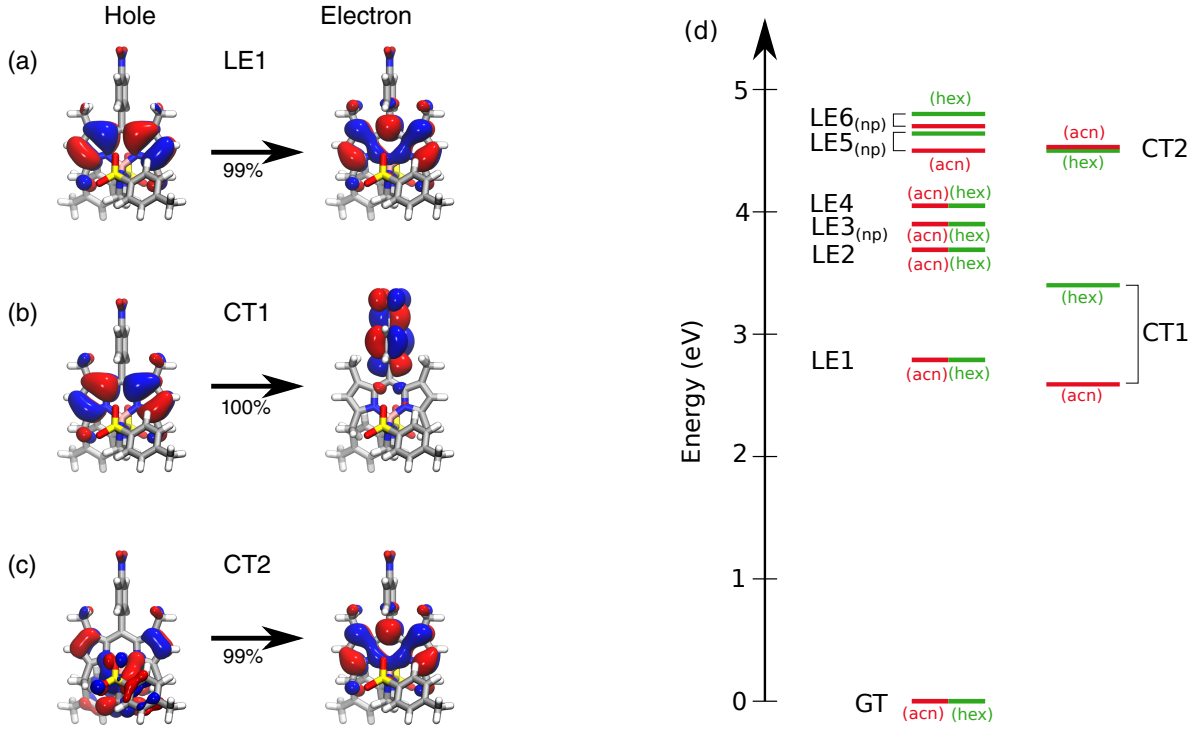

Figure 10: *a-c) Dominant natural transition orbital pairs for (a) the first locally excited state and (b,c) the first two charge-transfer states of N-BODIPY* **1**. *The percentage below the arrow indicates the weight of the dominant NTO pair in the transition. d) Scheme of the computed energy levels involved in the observed ultrafast dynamics, corrected for the reorganization energy. Red and green lines indicates energy levels computed in acetonitrile and n-hexane, respectively. The subscript* (np) *indicates states localized on the nitrophenyl moiety.*

involved in the transient dynamics starting from the lowest bright state.

Ray et al. have suggested that a charge-transfer state like CT2 might be responsible for the low quantum yield of some N-BODIPYs [59]. However, the N-BODIPYs with reduced quantum yield possess a benzo-fused diamino-boron moiety. The absence of the aryl ring makes the CT2 state too high in energy to contribute to the dynamics.

In order to understand the influence of the CT1 state on the excited-state dynamics, we considered the effect of solvent reorganization after charge separation, by computing the energy of the CT1 state with acetonitrile solvent in complete equilibrium (see Computational Methods). The equilibrium-solvation CT1 energy is 2.69 eV, lower than the bright BODIPY excited state. Namely, when the solvent relaxes around the charge-separated state, its energy drops below the bright state, making charge separation thermodynamically favoured ($\Delta G = -0.12$ eV). The solvent reorganization energy is estimated to be $\lambda = 0.63$ eV by subtracting the nonequilibrium and equilibrium solvation results. On the contrary, the reorganization energy in hexane solution is negligible, and the CT1 state is located above the LE1 state in energy, in agreement with the experimental results, which show a less pronounced CT state contribution in the observed dynamics in non polar solvents. A scheme of the computed energetic levels involved on the observed excited state dynamics is represented in Fig. 10d, corrected for the reorganization energy.

The computed excited state energies also allow to give a possible explanation about the kinetic behavior observed for the studied molecule when excited at 350 nm. Indeed several excited states are found which are completely localized on the nitrophenyl substituent. In particular, the LE3 state could be accessed if excitation at 350 nm populates the LE4 state (which is possible, considering the error on the computed excited state energies). Being completely localized on the *meso* substituent, which is arranged perpendicular to the BODIPY core, it is expected that this state is only weakly coupled with the low lying LE1 state, as confirmed by the computed couplings in SI (Tab. S2). This can explain the observed slower excited state recovery upon excitation at 350 nm and the appearance of the blue shifted fluorescence band, as due to this localized state.

4. Conclusions

In conclusion, we fully investigated the ultrafast behavior of a substituted N-BODIPY, a class of compounds that was not explored in depth in literature before. We found that the excited state dynamics of this molecule is highly dependent on the solvent polarity and on the excitation wavelength. By combining the experimental results from stationary and ultrafast spectroscopy with theoretical TD-DFT calculations, we conclude that both charge transfer and localized states

are involved in the photodynamics, to a different extent depending on both solvent and excitation conditions. Based on previous literature, we identify the transient signals of a radical cation localized on the BODIPY core, which is particularly evident in polar solvents. TD-DFT computations support the involvement of charge transfer states in the deactivation process of the molecule, since a low energy excited state is found, involving a charge transfer from the BODIPY core to the *meso* nitrophenyl substituent. This state is particularly stabilized in polar solvents and the occurrence of photoinduced electron transfer is responsible for the drastic decrease in the fluorescence quantum yield observed in polar solvents. Furthermore we found an unusually longer excited state lifetime upon excitation at 350 nm, if compared with that registered upon 500 nm excitation. This behaviour is rationalized by considering that the excited state relaxation upon excitation at higher energies involves the population of excited states completely localized on the *meso* nitrophenyl substituent, weakly coupled with the low lying excited state localized on the N-BODIPY core.

This work represents a starting point toward the comprehension of the photoinduced processes structure-properties relationships of N-BODIPY compounds, opening the possibility of tuning their electronic properties to optimize their performance in a number of applications, from light-harvesting to chemosensors and optoelectronic devices.

Declaration of competing interest

The authors declare that they have no known competing financial interests or personal relationships that could have appeared to influence the work reported in this paper.

Acknowledgement

The authors thank the European Union's Horizon 2020 research and innovation program under grant agreement n. 871124 Laserlab-Europe.

The authors also thank Dr Lorenzo Zani, Dr Massimo Calamnte and Dr Alessio Dessì from ICCOM-CNR in Sesto Fiorentino (FI), for support in the quantum yield measurements.

LC thanks the funding by the European Research Council, under the grant ERC-AdG-786714 (LIFETimeS).

References

[1] Ulrich, G., Ziessel, R., Harriman, A.. The chemistry of fluorescent bodipy dyes: Versatility unsurpassed. Angewandte Chemie International Edition 2008;47(7):1184–1201.

[2] Benniston, A.C., Copley, G.. Lighting the way ahead with boron dipyrromethene (bodipy) dyes. Phys Chem Chem Phys 2009;11:4124–4131.

[3] Baruah, M., Qin, W., Basarić, N., De Borggraeve, W.M., Boens, N.. Bodipy-based hydroxyaryl derivatives as fluorescent ph probes. The Journal of Organic Chemistry 2005;70(10):4152–4157.

[4] Bañuelos, J.. Bodipy dye, the most versatile fluorophore ever? The Chemical Record 2016;16(1):335–348.

[5] Boens, N., Leen, V., Dehaen, W.. Fluorescent indicators based on bodipy. Chem Soc Rev 2012;41:1130–1172.

[6] Ni, Y., Wu, J.. Far-red and near infrared bodipy dyes: synthesis and applications for fluorescent ph probes and bio-imaging. Org Biomol Chem 2014;12:3774–3791.

[7] Lu, H., Mack, J., Yang, Y., Shen, Z.. Structural modification strategies for the rational design of red/nir region bodipys. Chem Soc Rev 2014;43:4778–4823.

[8] Belmonte-Vázquez, J.L., Avellanal-Zaballa, E., Enríquez-Palacios, E., Cerdán, L., Esnal, I., Bañuelos, J., et al. Synthetic approach to readily accessible benzofuran-fused borondipyrromethenes as red-emitting laser dyes. The Journal of Organic Chemistry 2019;84(5):2523–2541.

[9] Costela, A., García-Moreno, I., Sastre, R.. Polymeric solid-state dye lasers: Recent developments. Phys Chem Chem Phys 2003;5:4745–4763.

[10] Benstead, M., Mehl, G.H., Boyle, R.W.. 4,4'-difluoro-4-bora-3a,4a-diaza-s-indacenes (bodipys) as components of novel light active materials. Tetrahedron 2011;67(20):3573 – 3601.

[11] Bañuelos, J., López Arbeloa, F., Arbeloa, T., Salleres, S., Amat-Guerri, F., Liras, M., et al. Photophysical study of new versatile multichromophoric diads and triads with bodipy and polyphenylene groups. J of Phys Chem A 2008;112(43):10816–10822.

[12] Lam, S., Damzen, M.. Self-adaptive holographic solid-state dye laser. Optics Communications 2003;218(4):365 – 370.

[13] Esnal, I., Duran-Sampedro, G., Agarrabeitia, A.R., Bañuelos, J., García-Moreno, I., Macías, M.A., et al. Coumarin–bodipy hybrids by heteroatom linkage: versatile, tunable and photostable dye lasers for uv irradiation. Phys Chem Chem Phys 2015;17:8239–8247.

[14] Otsuka, T., Takahashi, N., Fujigasaki, N., Sekine, A., Ohashi, Y., Kaizu, Y.. Crystal structure and energy transfer in double-complex salts composed of tris(2,2'-bipyridine)ruthenium(ii) or tris(2,2'-bipyridine)osmium(ii) and hexacyanochromate(iii). Inorganic Chemistry 1999;38(6):1340–1347.

[15] Badré, S., Monnier, V., Méallet-Renault, R., Dumas-Verdes, C., Schmidt, E.Y., Mikhaleva, A.I., et al. Fluorescence of molecular micro- and nanocrystals prepared with bodipy derivatives. Journal of Photochemistry and Photobiology A: Chemistry 2006;183(3):238 – 246.

[16] Ziessel, R., Ulrich, G., Harriman, A.. The chemistry of bodipy: A new el dorado for fluorescence tools. New J Chem 2007;31:496–501.

[17] Ziessel, R., Harriman, A.. Artificial light-harvesting antennae: electronic energy transfer by way of molecular funnels. Chem Commun 2011;47:611–631.

[18] Bozdemir, O.A., Cakmak, Y., Sozmen, F., Ozdemir, T., Siemiarczuk, A., Akkaya, E.U.. Synthesis of symmetrical multichromophoric bodipy dyes and their facile transformation into energy transfer cassettes. Chemistry – A European Journal 2010;16(21):6346–6351.

[19] D'Souza, F., Smith, P.M., Zandler, M.E., McCarty, A.L., Itou, M., Araki, Y., et al. Energy transfer followed by electron transfer in a supramolecular triad composed of boron dipyrrin, zinc porphyrin, and fullerene: A model for the photosynthetic antenna-reaction center complex. Journal of the American Chemical Society 2004;126(25):7898–7907.

[20] Imahori, H., Norieda, H., Yamada, H., Nishimura, Y., Yamazaki, I., Sakata, Y., et al. Light-harvesting and photocurrent generation by gold electrodes modified with mixed self-assembled monolayers of boron-dipyrrin and ferrocene-porphyrin-fullerene triad. J Am Chem Soc 2001;123(1):100–110.

[21] D'Souza, F., Smith, P., Zandler, M., McCarty, A., Itou, M., Araki, Y., et al. Energy transfer followed by electron transfer in a supramolecular triad composed of boron dipyrrin, zinc porphyrin, and fullerene: a model for the photosynthetic antenna-reaction center complex. J Am Chem Soc 2004;126(25):7898–7907.

[22] Fan, J., Hu, M., Zhan, P., Peng, X.. Energy transfer cassettes based on organic fluorophores: construction and applications in ratiometric sensing. Chem Soc Rev 2013;42:29–43.

[23] Ziessel, R., Ulrich, G., Haefele, A., Harriman, A.. An artificial light-harvesting array constructed from multiple bodipy dyes. Journal

of the American Chemical Society 2013;135(30):11330–11344.

[24] Lu, J.s., Fu, H., Zhang, Y., Jakubek, Z.J., Tao, Y., Wang, S.. A dual emissive bodipy dye and its use in functionalizing highly monodispersed pbs nanoparticles. Angew Chem Int Ed 2011;50(49):11658–11662.

[25] Bessette, A., Hanan, G.S.. Design, synthesis and photophysical studies of dipyrromethene-based materials: insights into their applications in organic photovoltaic devices. Chem Soc Rev 2014;43:3342–3405.

[26] Marcus, R.A.. Electron transfer reactions in chemistry. theory and experiment. Rev Mod Phys 1993;65:599–610.

[27] Fox, M., Chanon, M.. Photoinduced electron transfer. parts a-d. Angew Chem 1990;102(4):460–462.

[28] Wasielewski, M.R.. Photoinduced electron transfer in supramolecular systems for artificial photosynthesis. Chem Rev 1992;92(3):435–461.

[29] Rurack, K., Resch-Genger, U.. Rigidization, preorientation and electronic decoupling - the 'magic triangle' for the design of highly efficient fluorescent sensors and switches. Chem Soc Rev 2002;31:116–127.

[30] Kowada, T., Maeda, H., Kikuchi, K.. Bodipy-based probes for the fluorescence imaging of biomolecules in living cells. Chem Soc Rev 2015;44:4953–4972.

[31] Sunahara, H., Urano, Y., Kojima, H., Nagano, T.. Design and synthesis of a library of bodipy-based environmental polarity sensors utilizing photoinduced electron-transfer-controlled fluorescence on/off switching. Journal of the American Chemical Society 2007;129(17):5597–5604.

[32] Koutaka, H., ichi Kosuge, J., Fukasaku, N., Hirano, T., Kikuchi, K., Urano, Y., et al. A novel fluorescent probe for zinc ion based on boron dipyrromethene (bodipy) chromophore. Chemical and Pharmaceutical Bulletin 2004;52(6):700–703.

[33] Werner, T., Huber, C., Heinl, S., Kollmannsberger, M., Daub, J., Wolfbeis, O.S.. Novel optical ph-sensor based on a boradiazaindacene derivative. J Anal Chem 1997;359:150–154.

[34] Koutaka, H., ichi Kosuge, J., Fukasaku, N., Hirano, T., Kikuchi, K., Urano, Y., et al. A novel fluorescent probe for zinc ion based on boron dipyrromethene (bodipy) chromophore. Chemical and Pharmaceutical Bulletin 2004;52(6):700–703.

[35] Gareis, T., Huber, C., S. Wolfbeis, O., Daub, J.. Phenol/phenolate-dependent on/off switching of the luminescence of 4,4-difluoro-4-bora-3a,4a-diaza-s-indacenes. Chem Commun 1997;:1717–1718.

[36] Batat, P., Vives, G., Bofinger, R., Chang, R.W., Kauffmann, B., Oda, R., et al. Dynamics of ion-regulated photoinduced electron transfer in bodipy-bapta conjugates. Photochem Photobiol Sci 2012;11:1666–1674.

[37] Trieflinger, C., Röhr, H., Rurack, K., Daub, J.. Multiple switching and photogated electrochemiluminescence expressed by a dihydroazulene/boron dipyrromethene dyad. Angew Chem Int Ed 2005;44(42):6943–6947.

[38] Gabe, Y., Ueno, T., Urano, Y., Kojima, H., Nagano, T.. Tunable design strategy for fluorescence probes based on 4-substituted bodipy chromophore: improvement of highly sensitive fluorescence probe for nitric oxide. Anal Bioanal Chem 2006;386(3):621–626.

[39] Antina, E.V., Bumagina, N.A., V'yugin, A.I., Solomonov, A.V.. Fluorescent indicators of metal ions based on dipyrromethene platform. Dyes and Pigments 2017;136:368 – 381.

[40] Sayre, L.M., Perry, G., Smith, M.A.. Redox metals and neurodegenerative disease. Curr Opin Chem Biol 1999;3(2):220–225.

[41] Beer, G., Niederalt, C., Grimme, S., Daub, J.. Redox switches with chiroptical signal expression based on binaphthyl boron dipyrromethene conjugates. Angew Chem Int Ed 2000;39(18):3252–3255.

[42] Heyne, B., Ahmed, S., Scaiano, J.C.. Mechanistic studies of fluorescent sensors for the detection of reactive oxygen species. Org Biomol Chem 2008;6:354–358.

[43] Benniston, A.C., Copley, G., Elliott, K.J., Harrington, R.W., Clegg, W.. Redox-controlled fluorescence modulation in a bodipy-quinone dyad. European Journal of Organic Chemistry 2008;2008(16):2705–2713.

[44] Yamada, Y., Tomiyama, Y., Morita, A., Ikekita, M., Aoki, S.. Bodipy-based fluorescent redox potential sensors that utilize reversible redox properties of flavin. Chembiochem 2008;2008(9):853–856.

[45] Sun, Z.N., Liu, F.Q., Chen, Y., Tam, P.K.H., Yang, D.. A highly specific bodipy-based fluorescent probe for the detection of hypochlorous acid. Organic Letters 2008;10(11):2171–2174.

[46] Kamkaew, A., Lim, S.H., Lee, H.B., Kiew, L.V., Chung, L.Y., Burgess, K.. Bodipy dyes in photodynamic therapy. Chem Soc Rev 2013;42:77–88.

[47] Awuah, S.G., You, Y.. Boron dipyrromethene (bodipy)-based photosensitizers for photodynamic therapy. RSC Adv 2012;2:11169–11183.

[48] Osati, S., Ali, H., van Lier, J.E.. Synthesis and spectral properties of phthalocyanine–bodipy conjugates. Tetrahedron Letters 2015;56(16):2049 – 2053.

[49] Ye, J., Ye, W., Xiao, C., Chen, Y., Wang, G., Zhang, W.. A new approach to the synthesis of β-formyl-boron-dipyrromethenes. Chin J Org Chem 2012;32:1503.

[50] Wang, P., Giese, R.W.. Phosphate-specific fluorescence labeling with bo-imi: reaction details. Journal of Chromatography A 1998;809(1):211 – 218.

[51] Kim, H., Burghart, A., B. Welch, M., Reibenspies, J., Burgess, K.. Synthesis and spectroscopic properties of a new 4-bora-3a,4a-diaza-s-indacene (bodipy®) dye. Chem Commun 1999;:1889–1890.

[52] Ulrich, G., Goze, C., Guardigli, M., Roda, A., Ziessel, R.. Pyrromethene dialkynyl borane complexes for "cascatelle" energy transfer and protein labeling. Angewandte Chemie International Edition 2005;44(24):3694–3698.

[53] Kee, H., Kirmaier, C., Yu, L., Thamyongkit, P., Youngblood, W., Calder, M., et al. Structural control of the photodynamics of boron-dipyrrin complexes. J Phys Chem B 2005;109(43):20433–20443.

[54] Duran-Sampedro, G., Agarrabeitia, A.R., Lopez, T.A., Bañuelos, J., López-Arbeloa, I., Chiara, J.L., et al. Increased laser action in commercial dyes from fluorination regardless of their skeleton. Laser Physics Letters 2014;11(11).

[55] Durán-Sampedro, G., Agarrabeitia, A.R., Cerdán, L., Pérez-Ojeda, M.E., Costela, A., García-Moreno, I., et al. Carboxylates versus fluorines: Boosting the emission properties of commercial bodipys in liquid and solid media. Advanced Functional Materials 2013;23(34):4195–4205.

[56] Duran-Sampedro, G., Esnal, I., Agarrabeitia, A.R., Bañuelos Prieto, J., Cerdán, L., García-Moreno, I., et al. First highly efficient and photostable e and c derivatives of 4,4-difluoro-4-bora-3a,4a-diaza-s-indacene (bodipy) as dye lasers in the liquid phase, thin films, and solid-state rods. Chemistry – A European Journal 2014;20(9):2646–2653.

[57] Duran-Sampedro, G., Agarrabeitia, A.R., Garcia-Moreno, I., Costela, A., Bañuelos, J., Arbeloa, T., et al. Chlorinated bodipys: Surprisingly efficient and highly photostable laser dyes. European Journal of Organic Chemistry 2012;2012(32):6335–6350.

[58] Lakshmi, V., Rajeswara Rao, M., Ravikanth, M.. Halogenated boron-dipyrromethenes: synthesis, properties and applications. Org Biomol Chem 2015;13:2501–2517.

[59] Ray, C., Díaz-Casado, L., Avellanal-Zaballa, E., Baũelos, J., Cerdán, L., Garcíía-Moreno, I., et al. N-bodipys come into play: Smart dyes for photonic materials. Chem Eur J 2017;23(39):9383–9390.

[60] Ray, C., Schad, C., Avellanal-Zaballa, E., Moreno, F., Bañuelos, J., Maroto, B.L., et al. Exploring n-bodipys as privileged scaffolds to build off/on fluorescent sensors by pet. Proceedings 2019;41(1):54.

[61] van Stokkum, I.H., Larsen, D.S., van Grondelle, R.. Global and target analysis of time-resolved spectra. Biochimica et Biophysica Acta (BBA) - Bioenergetics 2004;1657(2):82 – 104.

[62] Henry, E., Hofrichter, J.. Singular value decomposition: Application to analysis of experimental data. In: Numerical Computer Methods; vol. 210 of *Methods in Enzymology*. Academic Press; 1992, p. 129 –

192.
[63] Snellenburg, J., Laptenok, S., Seger, R., Mullen, K., van Stokkum, I.. Glotaran: A java-based graphical user interface for the r package timp. Journal of Statistical Software, Articles 2012;49(3):1–22.
[64] Chai, J.D., Head-Gordon, M.. Systematic optimization of long-range corrected hybrid density functionals. J Chem Phys 2008;128(8):084106.
[65] Chai, J.D., Head-Gordon, M.. Long-range corrected hybrid density functionals with damped atom–atom dispersion corrections. Phys Chem Chem Phys 2008;10(44):6615.
[66] Iikura, H., Tsuneda, T., Yanai, T., Hirao, K.. A long-range correction scheme for generalized-gradient-approximation exchange functionals. J Chem Phys 2001;115(8):3540–3544.
[67] Dreuw, A., Weisman, J.L., Head-Gordon, M.. Long-range charge-transfer excited states in time-dependent density functional theory require non-local exchange. J Chem Phys 2003;119(6):2943–2946.
[68] Vydrov, O.A., Scuseria, G.E.. Assessment of a long-range corrected hybrid functional. J Chem Phys 2006;125:234109.
[69] Dreuw, A., Head-Gordon, M.. Single-reference ab initio methods for the calculation of excited states of large molecules. Chem Rev 2005;105(11):4009–37.
[70] Martin, R.L.. Natural transition orbitals. J Chem Phys 2003;118(11):4775–4777.
[71] Guido, C.A., Cortona, P., Adamo, C.. Effective electron displacements: A tool for time-dependent density functional theory computational spectroscopy. J Chem Phys 2014;140(10).
[72] Caricato, M., Mennucci, B., Tomasi, J.. Formation and relaxation of excited states in solution: A new time dependent polarizable continuum model based on time dependent density functional theory. J Chem Phys 2006;124(12):124520.
[73] Nottoli, M., Jurinovich, S., Cupellini, L., Gardiner, A.T., Cogdell, R., Mennucci, B.. The role of charge-transfer states in the spectral tuning of antenna complexes of purple bacteria. Photosynth Res 2018;137(2):215–226.
[74] Zhao, C., Feng, P., Cao, J., Zhang, Y., Wang, X., Yang, Y., et al. 6-hydroxyindole-based borondipyrromethene: Synthesis and spectroscopic studies. Org Biomol Chem 2012;10:267–272.
[75] Benniston, A.C., Clift, S., Hagon, J., Lemmetyinen, H., Tkachenko, N.V., Clegg, W., et al. Effect on charge transfer and charge recombination by insertion of a naphthalene-based bridge in molecular dyads based on borondipyrromethene (bodipy). ChemPhysChem 2012;13(16):3672–3681.
[76] Guennic, B.L., Jacquemin, D.. Taking up the cyanine challenge with quantum tools. Acc Chem Res 2015;48(3):530–537.